The effect of harvesting on biomass production and nutrient removal in phototrophic biofilm reactors for effluent polishing

N. C. Boelee · M. Janssen · H. Temmink ·
L. Taparavičiūtė · R. Khiewwijit · Á. Jánoska ·
C. J. N. Buisman · R. H. Wijffels

Abstract An increasing number of wastewater treatment plants require post-treatment to remove residual nitrogen and phosphorus. This study investigated various harvesting regimes that would achieve consistent low effluent concentrations of nitrogen and phosphorus in a phototrophic biofilm reactor. Experiments were performed in a vertical biofilm reactor under continuous artificial lighting and employing artificial wastewater. Under similar conditions, experiments were performed in near-horizontal flow lanes with biofilms of variable thickness. It was possible to maintain low nitrogen and phosphorus concentrations in the effluent of the vertical biofilm reactor by regularly harvesting half of the biofilm. The average areal biomass production rate achieved a 7 g dry weight m^{-2} day^{-1} for all different harvesting frequencies tested (every 2, 4, or 7 days), corresponding to the different biofilm thicknesses. Apparently, the biomass productivity is similar for a wide range of biofilm thicknesses. The biofilm could not be maintained for more than 2 weeks as, after this period, it spontaneously detached from the carrier material. Contrary to the expectations, the biomass production doubled when the biofilm thickness was increased from 130 μm to 2 mm. This increased production was explained by the lower density and looser structure of the 2 mm biofilm. It was concluded that, concerning biomass production and labor requirement, the optimum harvesting frequency is once per week.

Keywords Microalgae · Harvesting · Biofilm thickness · Wastewater treatment · Nitrogen removal · Phosphorus removal

N. C. Boelee · M. Janssen · H. Temmink · L. Taparavičiūtė ·
R. Khiewwijit · Á. Jánoska · C. J. N. Buisman
Wetsus-Centre of Excellence for Sustainable Water Technology,
P.O. Box 1113, 8900 CC Leeuwarden, The Netherlands

N. C. Boelee · M. Janssen · R. H. Wijffels
Bioprocess Engineering, AlgaePARC, Wageningen University,
PO Box 8129, 6700 EV Wageningen, The Netherlands

N. C. Boelee (✉) · H. Temmink · C. J. N. Buisman
Sub-department of Environmental Technology, Wageningen
University, P.O. Box 8129, 6700 EV Wageningen, The Netherlands
e-mail: nadine.boelee@wetsus.nl
URL: www.AlgaePARC.com

Introduction

Microalgal biofilms can be applied for wastewater treatment and post-treatment of wastewater effluents to remove nitrogen (N) and phosphorus (P) (Boelee et al. 2012). As in all phototrophic systems, microalgal biofilms exhibit the potential to recover the N and P incorporated in the produced microalgal biomass. Biofilm systems also possess several advantages over suspended systems. First, biofilm systems are able to perform during shorter hydraulic retention times, and, secondly, it is easier to harvest the biomass from biofilm systems than from suspended systems. In addition, the microalgae in the biofilm are protected from pollutants due to diffusional gradients (Godos et al. 2009; Sabater et al. 2002). While suspended microalgal systems experience a high energy input (Norsker et al. 2011), biofilm systems are expected to demand less energy due to the easier harvesting and the absence of mixing (Ozkan et al. 2012). Finally, the evaporation of the water from the biofilm can be considered a disadvantage of biofilm systems although this evaporation also cools the biofilm, preventing the temperature in the biofilm from becoming too high (Murphy and Berberoğlu 2012).

Microalgal biofilm systems can be applied as post-treatment of municipal wastewater when the discharge of N and P must be reduced as a consequence of stricter regulations such as the EU Water Framework Directive. In concordance

with this directive, the N and P concentrations must be reduced from the current European discharge requirements of 10 mg N L^{-1} and 1 mg P L^{-1} to concentrations appropriate for discharge to 'sensitive' water bodies. Current Dutch guidelines for these sensitive water bodies are 2.2 mg L^{-1} total N and 0.15 mg L^{-1} total P. Laboratory studies have demonstrated that microalgal biofilms are able to remove N and P from wastewater effluent at removal rates of 0.1–1.3 g N m^{-2} day^{-1} and 0.006–0.19 g P m^{-2} day^{-1} (González et al. 2008; Godos et al. 2009; Boelee et al. 2011) and can attain effluent concentrations below the target values mentioned above (Boelee et al. 2011).

Generally, the growth of phototrophic biofilms follows a two-phase pattern. The first phase is the growth phase which begins with the colonization of the carrier material often by diatoms and green algae (Biggs 1996; Johnson et al. 1997). The biomass initially grows exponentially and, later, linearly, and the community evolves toward filamentous green algae and cyanobacteria (Biggs 1996; Johnson et al. 1997; Sekar et al. 2002). Biofilm growth subsequently decreases, and at a certain biofilm thickness, the growth becomes equal to the losses experienced through respiration, cell death, parasitism, disease, and grazing. This initiates the beginning of the second phase, the loss phase, where losses exceed growth (Biggs 1996).

When applying microalgal biofilms for wastewater treatment, the biofilm should be continuously maintained in the exponential or linear growth phase. This ensures a high biomass production and, thereby, a high nutrient removal rate. Regular harvesting of the biofilm can maintain the biofilm in the growth phase by preventing the biofilm from reaching the thickness at which the loss phase begins. When harvesting the biofilm, a fraction of the biomass should remain on the carrier material to allow continuous growth and removal of nutrients. This can, for instance, be achieved by employing scraping as a harvesting technique (Johnson and Wen 2009; Ellwood et al. 2011). However, only minimal attention has been paid to harvesting microalgal biofilms, and therefore, it is uncertain what amount of the biofilm should be harvested and at what frequency this harvesting should occur.

The aim of this study was to assess the fraction of a phototrophic biofilm that should be harvested and the frequency of harvesting required to maintain effluent concentrations below 2.2 mg N L^{-1} and 0.15 mg P L^{-1}. A comparison was conducted between harvesting the entire biofilm surface and harvesting only half of the biofilm back to the carrier material. In addition, the effect of three different harvesting frequencies was determined on the biomass production rate and on the N and P effluent concentrations in a vertical phototrophic biofilm reactor. Finally, the hypothesis that biomass productivity decreases with increasing biofilm thickness was investigated in horizontal flow lanes with biofilms of 130, 250, 500 μm, 1, and 2 mm.

Materials and methods

Vertical phototrophic biofilm reactor

Figures 1a and 2 depict the vertical phototrophic biofilm reactor employed in this study. The biofilm was grown on a 0.125 m^2 layer of Polyfelt Geolon PE180 (TenCate Geosynthetics, The Netherlands), a polyethylene-based woven geotextile. This layer was situated on top of a layer of Polyfelt P120, a polypropylene-based nonwoven geotextile (TenCate Geosynthetics), and both layers were fixed to a polypropylene support plate. To obtain a homogeneous liquid distribution, a flexible tube (Masterflex Norprene L/S 16, Cole-Parmer, USA) was positioned above the polypropylene plate 5 mm above the biofilm. This tube was cut along its length such that the liquid dripped from the tube onto the biofilm, resulting in a completely wet biofilm. A gutter placed below the biofilm collected the liquid which was then pumped to a 400 mL recycle vessel. In this vessel, the pH was measured and controlled at pH 7 by a pulse-wise addition of CO_2 gas. This CO_2 addition resulted in an average inorganic carbon concentration in the effluent of 10.5 mg L^{-1}, corresponding to 8.53 mg L^{-1}bicarbonate (HCO_3^-) at pH 7. The liquid, with an average temperature of 21 °C, was recycled at 170 mL min^{-1} and mixed with the inflow of 7 mL min^{-1} synthetic wastewater. The overflow of the recycle vessel resulted in the effluent of the biofilm reactor. This effluent was amassed and stored in the dark at 2 °C for a maximum of 24 h to determine the dry weight concentration of the suspended biomass. To prevent microalgal growth outside of the Polyfelt layer, the gutter featured a polypropylene cover, all tubing was black, glassware was brown, and all glassware and connections were covered in aluminum foil.

The phototrophic biofilm was continuously illuminated by a bank of four compact fluorescent lamps (MASTER PL-L Polar 36 W/840/4P, Phillips, The Netherlands) at an average light intensity of 180 μmol photons m^{-2} s^{-1}. The light intensity was measured with a 2π PAR quantum sensor (SA190, LI-COR Biosciences, USA) arranged at the level of the biofilm surface. Nutrient loading rates of 0.8 g N m^{-2} day^{-1} and 0.08 g P m^{-2} day^{-1} were selected (Table 1) which were comparable to previous work where maximum uptake capacities of 1.0 g N m^{-2} day^1 and 0.13 g P m^{-2} day^{-1} were determined at 220 μmol photons m^{-2} s^{-1} (Boelee et al. 2011).

Horizontal flow lanes

The flow lane biofilm reactor (Ontwikkelwerkplaats WUR, The Netherlands) is schematically illustrated in Fig. 1b. This flow lane reactor had five parallel 80 cm long and 3.5 cm wide flow lanes. The five flow lanes had edges of 3.5 mm on both sides and depths of 130, 250, 500 μm, 1, and 2 mm. The flow lanes were separated by vertical side walls with a height of 1.5 cm.
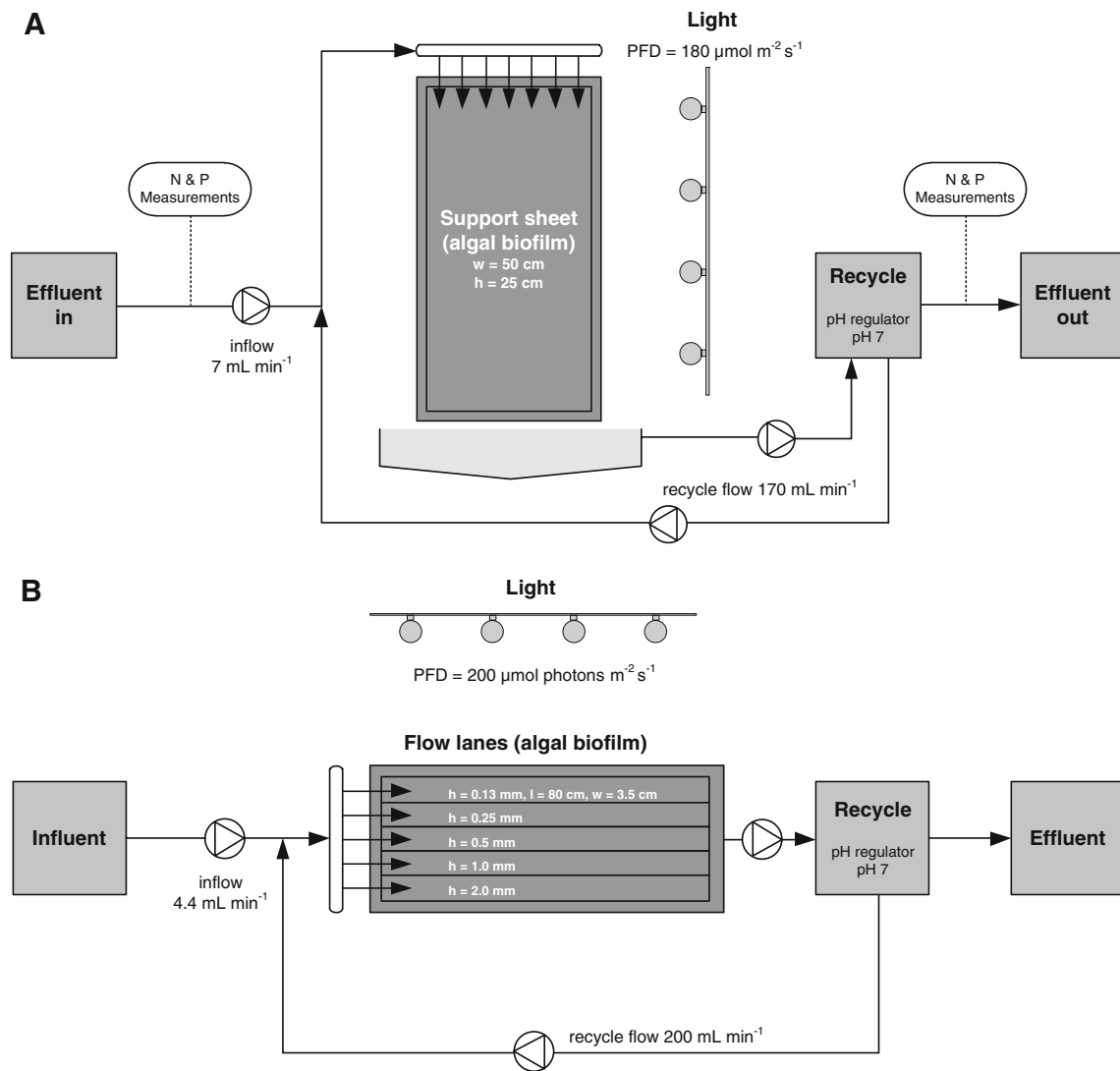
Fig. 1 Schematic overview of the vertical phototrophic biofilm reactor (**a**) and of the horizontal flow lane setup (**b**)

Synthetic wastewater entered a rotatable container positioned above the flow lanes with a flow rate of 4.4 mL min^{-1}. While the container was filling, the center point of gravity changed, and the container rotated when filled causing a wave to roll over the flow lanes. The flow lane setup was positioned at an angle of 4° to enable the liquid to flow over the lanes. The liquid, with an average temperature of 24 °C, was collected at the end of the lanes and pumped to a 400 mL recycle vessel. In this vessel, the pH was measured and controlled at pH 7 by a pulse-wise addition of CO_2 gas. From the recycle vessel, a recycle flow of 200 mL min^{-1} was combined with the influent and returned to the rotatable container. The overflow of the recycle vessel resulted in the effluent of the system.

The phototrophic biofilms in the flow lanes were continuously illuminated by LED light (FYTO Panel–Model B cool white LEDs, 280 pc, PSI, Czech Republic). Employing a light controller (Light Controller LC 150, PSI, Czech Republic),

the light intensity was specified at 200 µmol photons m^{-2} s^{-1}. The light intensity was measured with a 2π PAR quantum sensor (SA190, LI-COR Biosciences, USA) situated at the level of the biofilm surface. Plates covered with aluminium foil were positioned at the sides of the flow lanes to produce a more uniform light distribution among the biofilms.

Microalgal biofilm cultivation

Microalgal biofilm material was scraped from the surface of a settling tank of the effluent of the municipal wastewater treatment plant in Leeuwarden, The Netherlands, and further cultivated on small PVC sheets as described in Boelee et al. (2011). During the experiments with the vertical biofilm reactor, the Polyfelt sheet was inoculated by rubbing it with the PVC sheets containing biofilm. The flow lanes were also inoculated by rubbing them with the PVC sheets containing biofilm and also
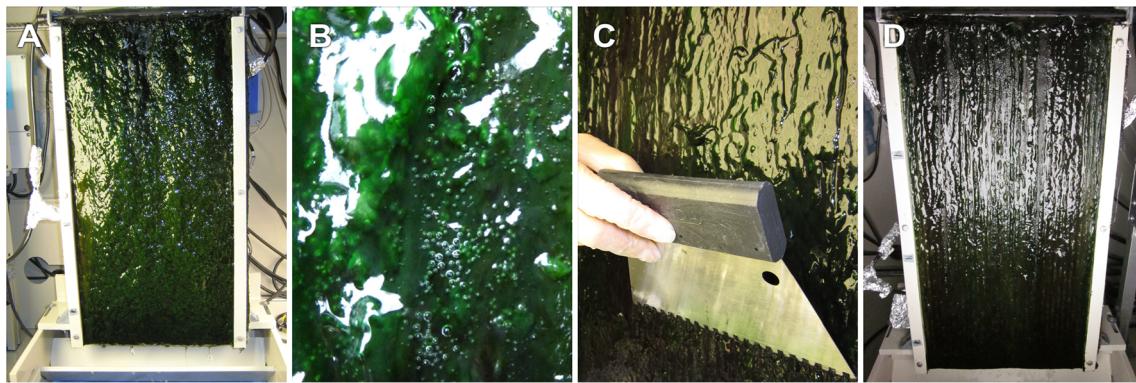
Fig. 2 The vertical phototrophic biofilm reactor (**a**), a close-up of the biofilm before harvesting (**b**), harvesting part of the biofilm with the adhesive comb (**c**), and the biofilm setup after harvesting (**d**)

by rubbing fresh biofilm material from the wastewater treatment plant in Leeuwarden over the bottom of the lanes.

The synthetic wastewater effluent supplied to the vertical biofilm reactor was designed to resemble the effluent from a typical municipal wastewater treatment plant and contained 10 mg L^{-1} NO_3^--N and 1.1 mg L^{-1} PO_4^{3-}-P. In addition, the synthetic wastewater contained (micro) nutrients based on Wright's cryptophyte medium (Andersen 2005) to rule out limitations of nutrients other than N or P. The synthetic wastewater lacked an organic carbon source in order to avoid heterotrophic growth. The synthetic wastewater composition of the vertical biofilm reactor was as follows—60.67 mg L^{-1} $NaNO_3$, 36.76 mg L^{-1} $CaCl_2.2H_2O$, 36.97 mg L^{-1} $MgSO_4.7H_2O$, 28.42 mg L^{-1} $Na_2SiO_3.9H_2O$, 6.19 mg L^{-1} K_2HPO_4. Trace elements and vitamins—3.82 mg L^{-1} $EDTA.2H_2O$, 1.90 mg L^{-1} $FeCl_3$, 10 µg L^{-1} $CuSO_4.5H_2O$, 22 µg L^{-1} $ZnSO_4.7H_2O$, 9.99 µg L^{-1} $CoCl_2.6H_2O$, 0.147 mg L^{-1} $MnCl_2.2H_2O$, 6.00 µg L^{-1} $Na_2MoO_4.2H_2O$, 1.00 mg L^{-1} H_3NO_3, 0.10 mg L^{-1} vitamin B1, 0.5 µg L^{-1} vitamin H, 0.5 µg L^{-1} vitamin B12.

The biofilms contained within the horizontal flow lanes were grown under light limitation by applying elevated nutrient concentrations at a high loading rate of 3.5 g N m^{-2} day^{-1} and 0.38 g P m^{-2} day^{-1}, as indicated in Table 1. In this manner, a dark zone may develop in the biofilm which will be accompanied by losses through respiration and cell death. The synthetic wastewater effluent of the horizontal flow lanes was as follows—442 mg L^{-1} $NaNO_3$, 268 mg L^{-1} $CaCl_2.2H_2O$, 269 mg L^{-1} $MgSO_4.7H_2O$, 207 mg L^{-1} $Na_2SiO_3.9H_2O$, 45.1 mg L^{-1} K_2HPO_4. Trace elements and vitamins—2.78 mg L^{-1} $EDTA.2H_2O$, 1.38 mg L^{-1} $FeCl_3$, 7.29 µg L^{-1} $CuSO_4.5H_2O$, 16 µg L^{-1} $ZnSO_4.7H_2O$, 7.27 µg L^{-1} $CoCl_2.6H_2O$, 0.107 mg L^{-1} $MnCl_2.2H_2O$, 4.37 µg L^{-1} $Na_2MoO_4.2H_2O$, 0.729 mg L^{-1} H_3NO_3, 0.0728 mg L^{-1} vitamin B1, 36.4 µg L^{-1} vitamin H, 36.4 µg L^{-1} vitamin B12.

Harvesting experiments

Three different experiments were performed: Experiments 1 and 2 in the vertical biofilm reactor and Experiment 3 in the horizontal flow lanes. Table 1 demonstrates the harvesting procedures that were followed during the three experiments. In Experiment 1, the entire biofilm was scraped from the 0.125 m^2 surface on days 26, 55, and 77 using a spatula, after which phototrophs could only have remained between the fibers of the Polyfelt material. In Experiment 2, a scraper was employed which was constructed from an adhesive comb. This scraper was designed to harvest half of the biofilm back to the Polyfelt material and was scraped over the biofilm from top to bottom, as illustrated in Fig. 2c. Harvesting occurred every 2, 4, or 7 days (Experiments 2A, 2B, and 2C). The biofilms in the flow lanes of Experiment 3 were harvested by running a blade over the edges of the flow lanes every day from Monday through Friday. In this manner, only the top layer of the biofilm was harvested, and the remaining biofilm

Table 1 The NO_3^--N and PO_4^{3-}-P loading rate, harvesting method and frequency of the three experiments

Experiment	Experimental setup	NO_3^--N loading rate (g m^{-2} day^{-1})	PO_4^{3-}-P loading rate (g m^{-2} day^{-1})	Harvesting method	Harvesting frequency
1	Vertical reactor	0.8	0.08	Scraping entire biofilm	Every ±20 days
2A	Vertical reactor	0.8	0.08	Scraping half of the biofilm	Every 2 days
2B	Vertical reactor	0.8	0.08	Scraping half of the biofilm	Every 4 days
2C	Vertical reactor	0.8	0.08	Scraping half of the biofilm	Every 7 days
3	Flow lanes	3.5	0.38	Scraping entire top of the biofilm	5 days per week

was of the thickness determined by the depth of the flow lanes (130, 250, 500 μm, 1, or 2 mm).

Analytical procedures

The NO_3^--N and PO_4^{3-}-P concentrations were monitored daily in the influent and effluent of the vertical biofilm reactor. In addition, the suspended solids were measured in the effluent every 3 days. Samples were extracted from the influent and effluent, filtered through a 0.45 μm filter (Millex-LCR, Merck Millipore, USA), and analyzed for NO_3^--N and PO_4^{3-}-P with ion chromatography (Compact IC 761, Metrohm, Switzerland). The Compact IC 761 was equipped with a conductivity detector with the pre-column Metrosep A Supp 4/5 Guard and with the column Metrosep A Supp 5, 150/4.0 mm (Metrohm). The collected effluent was filtered through pre-weighed glass fiber filters (GF/F, Whatman, UK) to determine the suspended dry weight. These filters were dried at 105 °C for at least 24 h.

To determine the dry weight of the harvested biomass, it was dried at 105 °C for at least 24 h. The harvested biomass was not washed with distilled water in order to prevent breakage of the cells. The biomass density of the wet biofilms was estimated from the volume of the wet biofilm and its dry weight content. In Experiment 2, the volume of the harvested biomass was measured in a graduated cylinder for each harvest. In Experiment 3, the volume of all five flow lanes was known, and, therefore, following the final harvest at the end of the experiment, all remaining biomass was removed from inside the flow lanes, and its dry weight was determined.

The C, N, and H content of dried and ground biomass was measured in duplicate with an elemental analyzer (EA 1110, ThermoQuest CE Instruments, USA) utilizing a vertical quartz tube (combustion tube) maintained at 1,000 °C with a constant flow of helium at 120 mL min^{-1}, an oxidation catalyst (WO_3) zone, a copper zone followed by a Porapack PQS column maintained at 60 °C, and finally, followed by a TCD detector. To determine the Ca, Fe, K, Mg, Na, P, S, and Si

content, duplicates of the biomass were digested using 10 mL HNO_3 (68 %) per 0.5 g dry biomass. During digestion, the temperature was increased over a 15-min duration until 180 °C was achieved in a microwave (ETHOS 1, Milestone, Italy) at 1,000 W, and these conditions were maintained for another 15 min. Following digestion, the concentrations of the elements were measured with inductive coupled plasma (Optima 5300 DV equipped with an optical emission spectrometer, Perkin Elmer, USA). The ash content was determined by burning the dried ground biomass at 550 °C for 2 h and dividing the ash weight by the dry weight.

Microscopy

Digital images of the biofilm were taken using a camera (Canon IXUS 105) and a Leica DM750 microscope (×400). The identification of microalgae was performed according to the Water quality-Guidance standard for the surveying, sampling, and laboratory analysis of phytobenthos in shallow running water (EN 15708) using an Olympus CX 31 microscope.

## Calculation of the elemental composition

The molar elemental composition of the biofilm, including oxygen, was calculated according to Duboc et al. (1999) using the measured weight of C, H, N, S, P, and ash.

Results

Biofilm growth in the vertical biofilm reactor

During Experiments 2A–C, the biofilm was green before harvesting while the underlying layer uncovered after harvesting was brown. The biofilm thickness varied over the surface, and gas bubbles of varying sizes were observed within the biofilm as depicted in Fig. 2b. Microscopic observations such as those demonstrated in Fig. 3 indicated that the

Fig. 3 *Phormidium* in the green top of the biofilm (**a**) and *Phormidium* together with other phototrophs in the browner bottom of the biofilm (**b**)
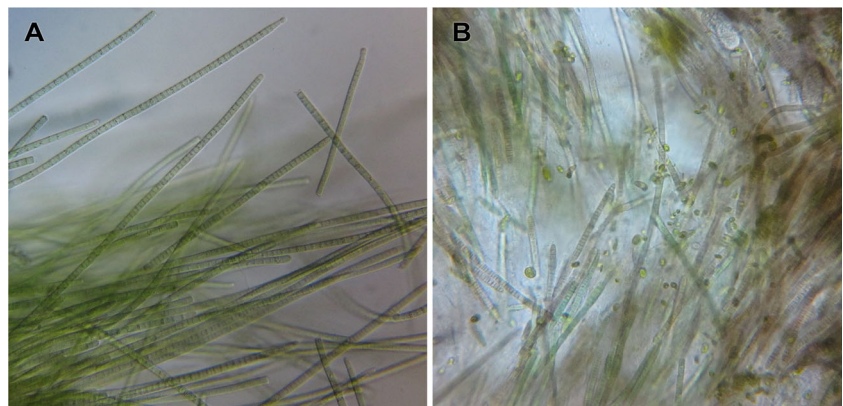
top layer of the biofilm consisted almost exclusively of the filamentous cyanobacterium *Phormidium*. This was in contrast to Experiment 1 where this cyanobacterium was not observed before or after harvesting the biofilm. A single dominating species is often observed in phototrophic biofilms, especially when the biofilm is growing fast (Zippel and Neu 2005) as was the case in these experiments. *Phormidium* is a well-known filamentous cyanobacterium that was also dominant in other studies (Johnson et al. 1997; Guzzon et al. 2008; Ellwood et al. 2011). In the bottom layer of the biofilms in Experiments 2A–C, different cyanobacteria and microalgae were also identified including the cyanobacteria *Pseudanabaena*, the diatom *Nitzschia,* and the green microalgae *Scenedesmus*. Species at the bottom of the biofilm have been suggested to be physiologically adapted to withstand prolonged exposure to light-limiting conditions (Johnson et al. 1997; Steinman and McIntire 1987). This pattern was consistently observed throughout Experiments 2A–C and is comparable with findings in other studies in artificial streams and biofilm incubators (Johnson et al. 1997; Guzzon et al. 2008).

Removal of NO_3^--N and PO_4^{3-}-P in the vertical biofilm reactor

Figure 4 depicts the concentrations of NO_3^--N and PO_4^{3-}-P in the effluent of the vertical biofilm system during Experiment 1. Until day 23, the NO_3^--N and PO_4^{3-}-P concentrations had only slightly decreased to 7.3 mg NO_3^--N L^{-1} and 0.36 mg PO_4^{3-}P L^{-1}. After the entire biofilm was harvested on day 26, the NO_3^--N and PO_4^{3-}-P concentrations decreased more rapidly. On day 37, the lowest concentrations were achieved of 0.66 mg NO_3^--N L^{-1} and 0.03 mg PO_4^{3-}P L^{-1}, after which the nutrient concentration began to increase. A similar pattern was observed following the subsequent two harvests, but the
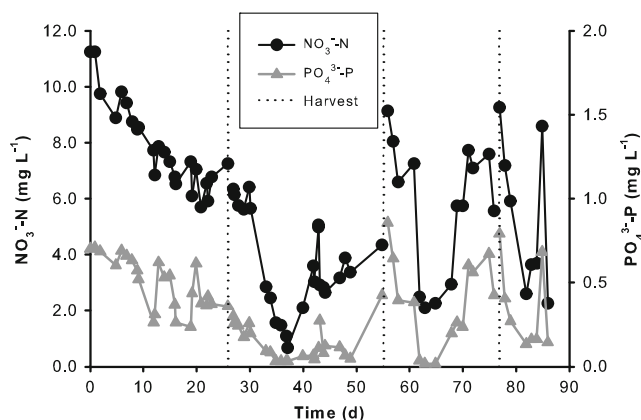
time required to achieve the lowest effluent concentrations shortened after each harvest—14 days after the first harvest,

Fig. 4 Effluent concentrations of NO_3^--N and PO_4^{3-}-P during Experiment 1 with an influent of 10 mg NO_3^--N L^{-1} and 1.0 mg PO_4^{3-}-P L^{-1}. The *dotted lines* indicate the time of harvest when the entire biofilm was scraped from the carrier material
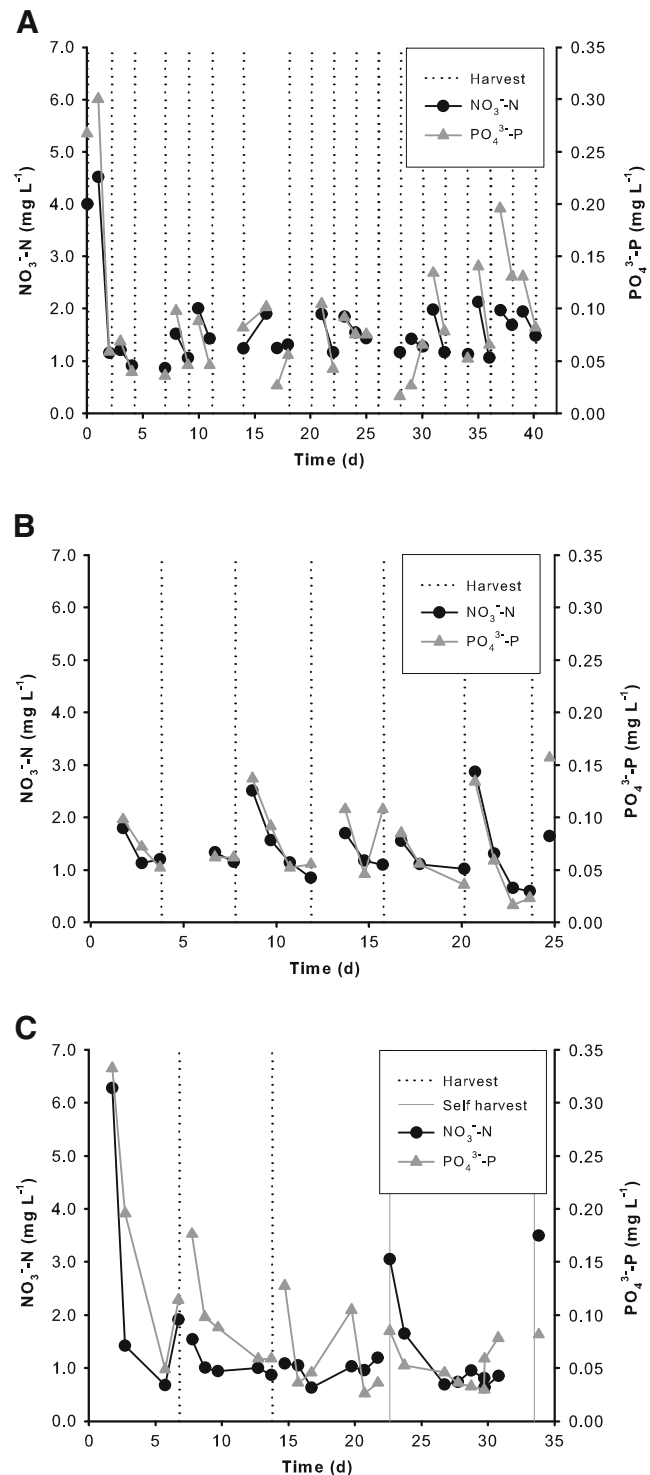
Fig. 5 Effluent concentrations of NO_3^--N and PO_4^{3-}-P during Experiment 2A (**a**), Experiment 2B (**b**), and Experiment 2C (**c**) with an influent of 10 mg NO_3^--N L^{-1} and 1.0 mg and PO_4^{3-}-P L^{-1}. The *dotted lines* (**a**–**c**) indicate the time of harvest when about half of the biofilm was scraped from the carrier material; the *grey line* (**c**) indicates the time when the biofilm fell from the carrier material
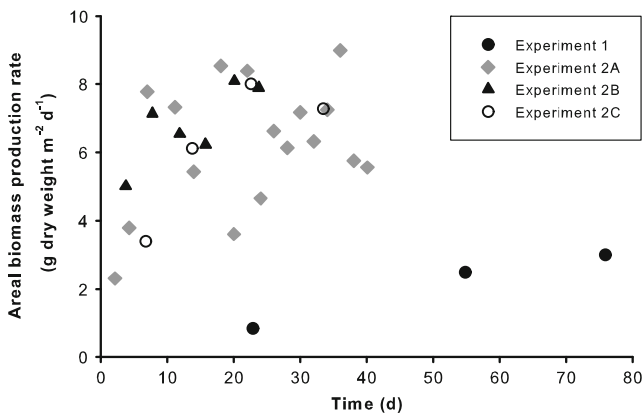
Fig. 6 The areal biomass production rates during Experiment 1 (harvesting the entire biofilm), Experiment 2A (harvesting every 2 days), 2B (harvesting every 4 days), and Experiment 2C (harvesting every 7 days)

8 days after the second, and only 6 days after the third. However, the NO_3^--N and PO_4^{3-}-P concentrations remained low for only a brief period of time.

Figure 5 presents the effluent concentrations of NO_3^--N and PO_4^{3-}-P during Experiments 2A–C when approximately half of the biofilm was harvested. The effluent concentrations remained low throughout the experiments and were, generally, below the target values of 2.2 mg N L^{-1} and 0.15 mg P L^{-1}. An increase in the NO_3^--N and PO_4^{3-}-P concentrations can be ascertained immediately after most harvests in Experiment 2A, and this increase became more evident at the lower harvesting frequencies in Experiments 2B and C.

Experiment 2C did not exhibit an increase in the effluent concentrations of NO_3^--N and PO_4^{3-}-P above the target values of 2.2 mg N L^{-1} and 0.15 mg P L^{-1} following the first two harvests. Therefore, it was decided to postpone the third harvest until the effluent concentrations increased above the target concentrations. Figure 5c indicates that, surprisingly, such an increase was not evidenced. After 9 days, the biofilm fell from the carrier material, and the same occurred after a consecutive growth period of 11 days.

Biomass production in the vertical biofilm reactor

Figure 6 illustrates that the areal biomass production rate was excessively variable during the experiments and that no clear differences were observed between the different harvesting frequencies of Experiments 2A–C. However, the areal biomass production rate in Experiment 1 whereby, the entire biofilm was harvested, was considerably lower than the production rates in Experiments 2A–C. For all harvesting regimes, the biomass production of the first one or two harvests was lower than the production of the later harvests.

The average areal biomass production rates of Experiments 1 and 2 are compared in Table 2. The average biomass production rate of Experiment 1 was 2.7 g dry weight m^{-2} day^{-1} while the average biomass production rate of Experiments 2A–C was 7 g dry weight m^{-2} day^{-1} (the first harvests were not taken into consideration). This biomass production, combined with the applied light intensity of 180 μmol photons m^{-2} s^{-1}, results in a biomass yield on light energy of 0.18 g dry weight mol^{-1} photons for Experiment 1 and of 0.43 and 0.46 g dry weight mol^{-1} photons for Experiments 2A and 2B–C.

Table 2 also demonstrates the water content of the biofilms which was determined at 90 % in Experiment 1 and 94 % in Experiments 2A–C. The ash content of the biomass ranged between 39 and 88 mg g^{-1} dry weight. The biofilm density was estimated from the measured volume and dry weight of the harvested biomass during Experiments 2A–C. The biofilm thickness was estimated based on the biofilm surface area, the measured volume of the harvested biomass, and the assumption that half of the biofilm was harvested. The biofilm density diminished with decreasing harvesting frequency or increasing biofilm thickness from 59 g dry weight L^{-1} at 500 μm to 31 g dry weight L^{-1} at 4.2 mm.

Mass balances N and P of the vertical biofilm reactor

Figure 7 provides the N and P mass balances for Experiments 1 and 2A–C. The average suspended dry weight

Table 2 The average areal biomass production rate, biomass yield on light energy, and the water content (measured as difference between wet and dry biomass) for Experiments 1 and 2, and the measured ash content and the estimated biofilm density and biofilm thickness for Experiment 2

Experiment	Areal biomass production rate (g dry weight m^{-2} day^{-1})	Yield (g dry weight mol photons^{-1})	Water content (%)	Biomass ash content (mg g^{-1} dry weight)	Estimated density (g dry weight L^{-1})	Estimated biofilm thickness (μm)
1	2.7 ($n=2$)	0.18	90 ($n=2$)			
2A	6.7 (±1.9 $n=17$)	0.43	94 (±0.8 $n=17$)	62 (±20 $n=4$)	59	500
2B	7.2 (±0.82 $n=5$)	0.46	94 (±0.007 $n=5$)	88 (±22 $n=3$)	47	1,300
2C	7.1 (±0.95 $n=3$)	0.46	94 (±1.6 $n=3$)	39 (±9 $n=3$)	31	4,200

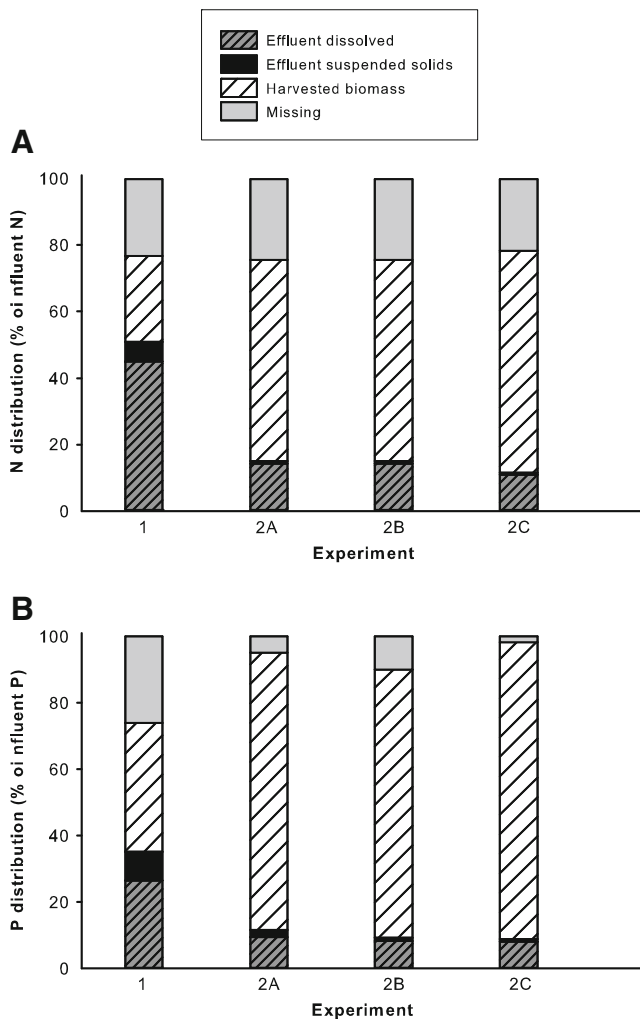In brackets, the standard deviation and the number of samples, n

Fig. 7 The mass balance for N (a) and for P (b). The mass balance shows the dissolved N or P in the effluent, the N or P in suspended solids in the effluent, the N or P in the harvested biomass, and the missing fraction as the percentage of the influent values for Experiments 1 and 2A–C

concentrations were 7.5 mg L^{-1} during Experiment 1; 1.4 mg L^{-1} during Experiment 2A; and 0.9 mg L^{-1} during Experiments 2B and 2C. It was assumed that the N and P content of these suspended solids was identical to the N and P content of the biomass in the biofilm. Figure 7 illustrates that only 1 % N and P departed from the system as suspended solids in the effluent in Experiments 2A–C. In Experiment 1, this was more extensive with 6 % N and 9 % P leaving the systems as suspended solids. The distribution of N and P was very similar in Experiments 2A–C where 63 % of N and 85 % of P was harvested with the biomass, and only 12 % of N and 9 % P departed from the reactor in a dissolved form with the effluent. In Experiment 1, only 26 % of N and 39 % of P was harvested with the biomass, and a major fraction of the nutrients left the reactor in dissolved form with the effluent (45 % N and 26 % P). The mass balances could not be completed as between 22 and 25 % of the N was unaccounted for and between 2 and 26 % of the P was unaccounted for.

Biofilm growth in the flow lanes

To investigate the effect of biofilm thickness on biomass production in more detail, in Experiment 3, biofilms were grown in flow lanes with varying thicknesses of 130, 250, 500 μm, 1, and 2 mm. The biofilms were harvested back to the default thickness 5 days a week. It proved difficult to harvest exactly to the default biofilm thickness as the biomass in the biofilms clung together resulting in often large patches of biofilm being harvested. This harvesting allowed sections of the flow lanes to be uncovered by the biofilms, as demonstrated in Fig. 8. Moreover, the structure of the thickest 2 mm biofilm in lane 5 was especially different from the other biofilms. This biofilm had a looser structure and contained more filamentous phototrophs and more gas bubbles.

Biomass production rates in the flow lanes

All five biofilms in the horizontal flow lanes of Experiment 3 had an area of 0.0266 m^2 available for phototrophic growth. Figure 9 presents the cumulative biomass produced in each flow lane. During the first 3 weeks (day 0–20), PO_4^{3-} precipitated in the influent supply vessel. Therefore, K_2HPO_4 was dissolved in a separate vessel and directly added to the system beginning on day 22. After day 22, the biomass production rate increased. The daily biomass production varied due to the uncontrolled harvesting described previously. Nevertheless, the cumulative biomass production exhibited the greatest biomass production of 398 g dry weight m^{-2} in the 2 mm biofilm and the lowest biomass production of 234 g dry weight m^{-2} in the 130 μm biofilm.

Table 3 shows the average areal biomass production rates between days 22 and 50. The biomass production rates of the two thinnest biofilms were 4.5 g dry weight m^{-2} day^{-1}. The other biofilms exhibited an increasing biomass production rate with thicker biofilms. The highest average areal biomass production rate of 9.9 g dry weight m^{-2} day^{-1} was attained with the 2 mm biofilm. From these production rates, the biomass yields on light energy were calculated between 0.26 and 0.57 g dry weight mol^{-1} photons. The biomass density of
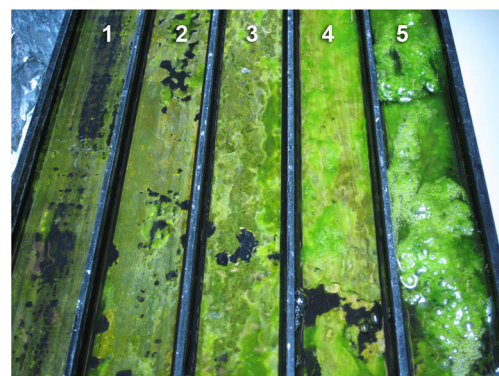

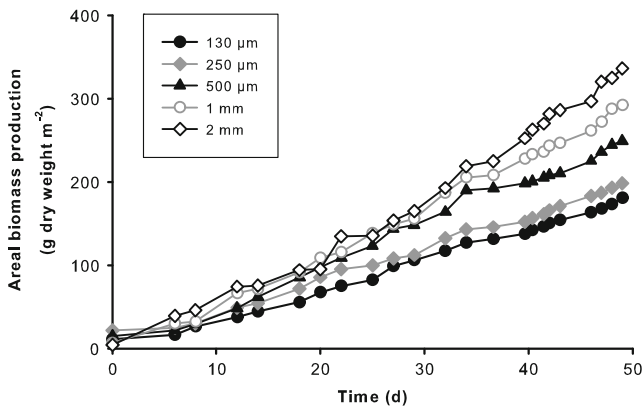Fig. 8 The biofilms in the flow lanes 1 (130 μm), 2 (250 μm), 3 (500 μm), 4 (1 mm), and 5 (2 mm)

Fig. 9 The cumulative biomass production of the biofilms 130 μm, 250 μm, 500 μm, 1 mm, and 2 mm (days 0–20 precipitation of PO_4^{3-} in the influent)

the five biofilms was determined at the end of the experiment when all biofilms were completely harvested. Table 3 indicates that this density decreased from 215 g dry weight L^{-1} at 250 μm to 37 g dry weight L^{-1} at 2 mm. The thinnest biofilm of 130 μm had a density of 104 g dry weight L^{-1}.

Elemental composition biomass

The elemental composition of the biomass was determined in order to construct the N and P mass balances depicted in Fig. 7. In Table 4, the composition of the biofilms harvested during Experiments 1–3 are compared with an average elemental composition of microalgae (Healey 1973). While the elemental composition of the biofilms of Experiments 1 and 2A–C was comparable to the composition in accordance to Healey (1973) and also to recently reported values in biofilm photobioreactors (Posadas et al. 2013), Experiment 3 exhibited an increased content of P, magnesium (Mg), and calcium (Ca). These extensive amounts of P, Mg, and Ca indicate that precipitation of calcium and magnesium phosphates occurred in the biofilm. This also corresponds with the low amount of carbon (C) in the biofilm material, indicating that less C was fixed than expected if the biofilm was constructed entirely of phototrophic biomass.

Table 3 The average areal biomass production rate from weeks 4–8, the average biomass yield on light energy, and the corresponding biofilm density for the biofilms of 130, 250, 500 μm, 1, and 2 mm

Biofilm thickness (μm)	Average areal biomass production rate (g dry weight m^{-2} day^{-1})	Yield (g dry weight mol photons^{-1})	Density (g dry weight L^{-1})
130	4.5	0.26	104
250	4.5	0.26	215
500	5.5	0.32	188
1,000	6.8	0.40	97
2,000	9.9	0.57	37

Table 4 The average elemental composition of the harvested biofilm for Experiment 1 and Experiment 2A–C and the elemental composition of the biomass from the final harvest of Experiment 3 as milligrams element per gram total dry weight

Experiment	C (mg g^{-1})	N (mg g^{-1})	H (mg g^{-1})	P (mg g^{-1})	K (mg g^{-1})	S (mg g^{-1})	Mg (mg g^{-1})	Fe (mg g^{-1})	Ca (mg g^{-1})	Na (mg g^{-1})	Si (mg g^{-1})	n
1	443	77.9	65.8	10.4	6.76	5.62	3.36	3.58	5.05	0.620	0.410	2
2A–C	450 (±8.7)	76.7 (±3.8)	66.8 (±2.0)	8.78 (±0.63)	8.84 (±0.81)	3.88 (±0.21)	2.85 (±0.20)	2.72 (±0.59)	1.99 (±0.20)	0.47 (±0.047)	0.222 (±0.074)[a]	10
3	304 (±24)	49.9 (±4.8)	44.9 (±1.7)	35.6 (±2.3)	5.35 (±1.1)	5.52 (±0.37)	31.5 (±14)	0.16 (±0.083)	81.0 (±7.3)	5.30 (1.4)	3.02 (±1.5)	5
Microalgae average	430	55	65	11	17.3	5.9	5.6	5.9	8.7	6.1	54	

In brackets the standard deviation, the average microalgae composition from (Healey 1973)

n.d. not determined, *n* number of samples

[a] The average only of the samples above the detection limit of 0.0662 mg g^{-1} (*n*=4)

The low Si content in all of the experiments implies that the number of diatoms in the biofilms was minimal.

Based on the elemental composition measurements and the ash measurement, the average molar elemental composition of the biomass in Experiment 2 was $C_1H_{1.77}O_{0.59}N_{0.15}P_{0.008}S_{0.0032}$, corresponding to a molar C/N/P ratio of 133:19:1. Whereas the H, N, and S content is comparable to other studies, the O content is high compared with the range of 0.40–0.47 reported by others (Hecky and Kilham [1988](#); Duboc et al. [1999](#); Kliphuis et al. [2010](#)). The N/P ratio is close to the ratio of 20:1 that was supplied and was also found previously by Boelee et al. ([2011](#)) employing identical wastewater effluent.

Discussion

When applying phototrophic biofilms as wastewater treatment, a thick biofilm is preferable as it requires less harvesting and results in more biomass per harvest. This study has demonstrated that the biomass production rates are comparable for biofilms harvested every 2, 4, or 7 days in a vertical biofilm reactor. Consequently, with similar biomass productions at different harvesting frequencies, the nutrient uptake rates and effluent concentrations obtained in a reactor with thick biofilms are comparable to a thin biofilm, while less labor is required and each harvest yields more biomass. Therefore, it will be optimal to maintain as extended time intervals as possible. With intervals exceeding 7 days, there is a risk of biofilm detachment which was emphasized in Experiment 2C. It is, therefore, concluded that the optimum harvesting frequency is once a week for a phototrophic biofilm reactor in which a section of the biofilm is harvested (as in this study). Within this period, the biofilm will remain stable and effluent concentrations will remain low.

This study investigated the hypothesis that biomass productivity decreases with increasing biofilm thickness. A low biomass production is undesirable as this will result in lower nutrient removal rates and higher nutrient effluent concentrations. The results of the vertical phototrophic biofilm reactor exhibited that the desired low effluent concentrations of 2.2 mg N L^{-1} and 0.15 mg P L^{-1} can only be obtained when harvesting half of the biomass but not when harvesting the entire biofilm. However, the results did not support the hypothesis of thicker biofilms being less productive as no differences were discovered between the areal biomass production rates with different harvesting frequencies (Experiment 2). In addition, the effluent N and P concentrations consistently remained below the target concentrations, though more frequent harvesting resulted in more stable effluent concentrations.

The hypothesis that an increasing biofilm thickness results in lower biomass production rates was also tested in more detail by growing biofilms of specific thicknesses under light limiting conditions (Experiment 3). The results demonstrated that the biomass production rate even increased with increasing biofilm

thickness, whereas the biomass density decreased with thicker biofilms. Furthermore, the thickest biofilm of 2 mm was found to have a more loose structure with more filamentous phototrophs compared with the thinner and denser biofilms. It is presumed that the light regimes experienced by the phototrophs were comparable for the thin and thick biofilms because the biofilm density approximately halved when the biofilm thickness doubled. This provides a similar number of phototrophs in the thin and thick biofilm and, therefore, a similar amount of light available for each phototroph. Therefore, the light regime was not responsible for the difference in biomass production between the different biofilm thicknesses.

The results suggest that the thickness of the biofilm affects its structure and, subsequently, its biomass production and nutrient uptake. In studies of bacterial biofilms, it was discovered that biofilms thicker than 400 μm had a lower density than thinner biofilms (Hoehn and Ray [1973](#); Bishop et al. [1995](#)). A biofilm with a lower density will presumably result in an increased flux of nutrients into the biofilm as a decrease in the biomass volume fraction results in a higher effective diffusive permeability (Stewart [1997](#)). Furthermore, the higher water content of a low density biofilm may enable more convection inside the biofilm, resulting in less diffusion limitations. In addition to the low density, the irregular surface of the thick biofilms in this study is also expected to provide lower mass transfer resistances and a higher diffusion rate of nutrients at the interface of the biofilm and the bulk liquid (De Beer et al. [1994](#); Wäsche et al. [2002](#)). Additional measurements of the O_2 profiles of the different biofilms determined that only the thick 2 mm biofilm had a profile which was constant at all depths with O_2 concentration of more than 100 % dissolved oxygen. This implies the presence of active phototrophs throughout the entire biofilm thickness, which corresponds with the assumed deep penetration of the nutrients. Cumulatively, the higher nutrient flux and deeper penetration of nutrients into thick biofilms with a low density appear to have led to increased biomass productions.

The biomass yield on light energy was almost equal at the different biofilm thicknesses of the vertical biofilm reactor in Experiment 2, ranging between 0.43 and 0.46 g dry weight mol^{-1} photons. The biomass yield on light energy ranged between 0.26 and 0.57 g dry weight mol^{-1} photons in the flow lanes of Experiment 3. In suspended microalgal cultures in photobioreactors, higher yields have been measured of 0.8 g dry weight mol^{-1} photons (Morita et al. [2000](#); Kliphuis et al. [2010](#)). A similar yield of 0.8 g dry weight mol^{-1} photons has also been considered possible for a vertical biofilm reactor (Boelee et al. [2012](#)) but was not achieved in this study. This lower biomass yield on light energy may have been caused by the PO_4^{3-} limitation in the biofilm. Nevertheless, the measured yields are higher than biomass yields on light energy measured in other biofilms setups of 0.15–0.27 g dry weight mol^{-1} photons at lower light intensities with monocultures of phototrophs (Johnson and Wen [2009](#); Ozkan et al. [2012](#)).

Table 5 The calculated penetration depths of NO_3^-, PO_4^{3-}, and HCO_3^- into the biofilm during Experiment 2 and of HCO_3^- when HCO_3^- in the water is in equilibrium with the air, in addition, the light intensity at each penetration depth for low light adapted to high light adapted phototrophs

Compound	Penetration depth (µm)	Light intensity at the penetration depth (µmol photons m^{-2} s^{-1})
NO_3^-	355	10–35
PO_4^{3-}	150	40–75
HCO_3^- (experiment)	250	20–50
HCO_3^- (air equilibrium)	25	125–150

Employing well-known models (e.g., described in (Pérez et al. 2005)), estimations were made of the penetration of light, CO_2, NO_3^-, and PO_4^{3-} into the biofilms of Experiment 2 (see Appendix, Penetration of NO_3^- PO_4^{3-} and HCO_3^-). Table 5 indicates that PO_4^{3-} had the smallest penetration depth of 150 µm, therefore, constituting the limiting nutrient. Light can also limit microalgal growth in the biofilm when the light intensity is lower than the compensation point, i.e., the light intensity at which the rate of photosynthesis is equal to the rate of respiration. This compensation point is reported to be between 8 and 40 µmol photons m^{-2} s^{-1} (Hill 1996; Clegg et al. 2012). At the penetration depth of the limiting nutrient (of PO_4), the light intensity was calculated to range between 40 and 75 µmol photons m^{-2} s^{-1} (see Appendix, Penetration of light) which is higher than the compensation point. It is, therefore, expected that PO_4^{3-} was indeed the limiting compound during Experiment 2. In this study, the synthetic wastewater was enriched with CO_2 for pH control, and the phototrophs were, therefore, not CO_2-limited. However, in the situation when CO_2 can only diffuse from the ambient air, CO_2 will constitute the limiting compound with a penetration depth of 25 µm. Therefore, CO_2 addition to the liquid will be required to maintain a high biomass production, unless the wastewater contains sufficient inorganic carbon to sustain microalgal growth (Van Vooren et al. 1999).

The estimated biofilm thicknesses in the vertical biofilm reactor (500 µm, 1.3, and 4.2 mm) are greater than the estimated penetration depths of light, CO_2, and nutrients. However, the actual biofilm thickness was even larger due to the gas bubbles which were entrapped in the biofilm and were discharged from the biofilm only during harvesting (and, thus, not included in the measurements). It was presumed that, at a certain biofilm thickness, the net phototrophic growth would decrease due to increased rates of endogenous respiration and cell death. Presumably, the time-scale of the experiments in this study had not been long enough to observe these losses.

The vertical phototrophic biofilm reactor achieved the desired low effluent concentrations of 2.2 mg N L^{-1} and 0.15 mg P L^{-1}. These measured effluent concentrations were not corrected for evaporation. While correction for evaporation

could result in even lower effluent concentrations, no correction will be made in full-scale systems. The loss of some water will not pose a problem in such full-scale systems as the final effluent be discharged to surface waters and not re-used. In addition, the evaporation of part of the wastewater provides an easy and efficient way to the cool the biofilm, which could otherwise get too warm during solar noon on sunny days (Murphy and Berberoğlu 2012).

Finally, for phototrophic biofilms in wastewater treatment, the method employed to supply the wastewater onto the biofilm is of great significance. The elemental composition of the biomass indicated the presence of precipitates in the biofilms of the flow lanes in Experiment 3, which is in contrast to the biofilms of the vertical reactor in Experiment 2. The precipitation in the flow lanes was most likely the result of the different manner of supplying liquid onto the biofilm between the two experiments. Whereas wastewater flowed continuously over the biofilm in the vertical reactor of Experiment 2, waves rolled over the biofilm in the horizontal flow lanes of Experiment 3 which may have resulted in a longer retention time of the liquid inside the biofilm. This longer retention time could have allowed the phototrophs to take up additional CO_2 and NO_3^- accompanied by a larger pH increase inside the biofilm. As precipitation of calcium or magnesium phosphates occurs at elevated pH, this may explain the precipitation that was detected in the biofilms within the flow lanes.
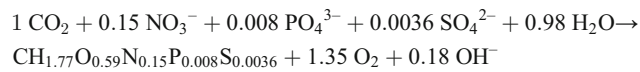
In conclusion, the present study has demonstrated that it was possible to continuously achieve effluent values below 2.2 mg N L^{-1} and 0.15 mg P L^{-1} employing a phototrophic biofilm reactor. To attain these low effluent values, it is necessary to frequently harvest a section of the biofilm but not the entire biofilm. The biomass productivity is optimal for a wide range of biofilm thicknesses as was indicated by the similar biomass production rate of 7 g dry weight m^{-2} day^{-1} when harvesting every 2, 4, or 7 days. Additional measurements in flow lanes demonstrated that, contrary to expectations, the areal biomass production rate increased with increasing biofilm thicknesses from 130 µm up to 2 mm. Nevertheless, it is expected that increasing the biofilm thickness further will eventually result in lower biomass production due to losses exceeding the biomass growth. The optimal harvesting frequency was determined to be once a week as the biofilm remains stable during this period (no self-detachment), and the system maintains low nutrient effluent concentrations.

Appendix

Penetration of NO_3^-, PO_4^{3-}, and HCO_3^-

The algal growth on NO_3^-, PO_4^{3-}, and CO_2 can be described by a stoichiometrical reaction equation. With the measured elemental composition of the biomass, this equation is as follows:

$$1\ CO_2 + 0.15\ NO_3^- + 0.008\ PO_4^{3-} + 0.0036\ SO_4^{2-} + 0.98\ H_2O \rightarrow$$
$$CH_{1.77}O_{0.59}N_{0.15}P_{0.008}S_{0.0036} + 1.35\ O_2 + 0.18\ OH^-$$

From this stoichiometrical growth equation, the yield of the different components can be calculated. The biomass content and the yields are shown in Table 6.

The penetration depths of NO_3^-, PO_4^{3-}, and HCO_3^- are calculated according to the following formula as described for instance in Perez et al. (2005):

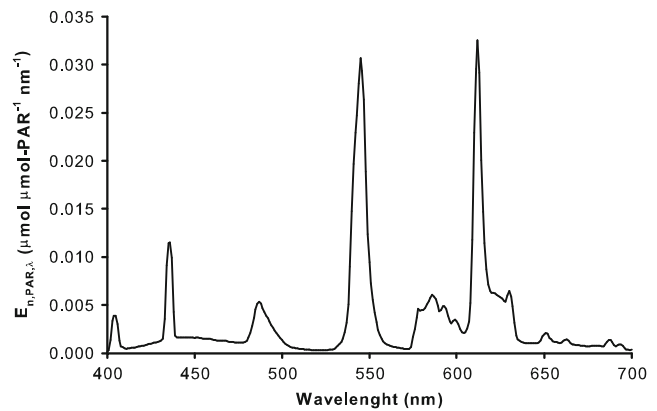$$L_{p,i} = \sqrt{\frac{2 \cdot D_i \cdot C_{i,l/b}}{\frac{\mu_{max}}{Y_i} \cdot C_x}}\ [m]$$

Fig. 10 The normalized spectral distribution of the PAR photons ($E_{n,PAR,\lambda}$ 400-700 nm) of the Phillips Master PL-L

with L_{pi} the penetration depth of nutrient i (meters), D_i the diffusion coefficient of nutrient i (square meters per second), $C_{i,l/b}$ the concentration of nutrient i at the liquid–biofilm interface (grams per cubic meter), μ_{max} the maximum specific growth rate (per second), Y_i the yield of biomass on nutrient i (gram biomass per gram nutrient i), and C_x the algae concentration (gram per cubic meter).

Table 6 shows the parameters that were used for the calculation. For the concentrations at the biofilm surface, it was

Table 6 Parameters for calculating the penetration depth of NO_3^-, $PO4^{3-}$, and HCO_3^- in the biofilm and parameters for calculating the light intensity at the penetration depths

Parameter	Value	Reference
$\Delta\lambda$	1	Chosen
μ_{max} (s^{-1})	1.2×10^{-5}	Average for *Phormidium* from Blier et al. (1995); Fujimoto and Sudo (1997); Talbot et al. (1991)
a_λ [a]	For *Chlorella sorokiniana*	
Biomass content	$C_1H_{1.77}O_{0.59}$ $N_{0.15}P_{0.008}S_{0.0036}$	Measured (average)
$C_{HCO3\ l/b}$ (g C m^{-3})	8.53	Calculated from the measured average total inorganic carbon of 10.5 mgL^{-1} at pH 7 during the experiment
	0.096	Calculated from the equilibrium value of CO_2 in water and air at pH 7
$C_{NO3\ l/b}$ (g N m^{-3})	2.2	Target value
$C_{PO4\ l/b}$ (g P m^{-3})	0.15	Target value
C_x (g m^{-3})	4.6×10^4	Measured (average)
d	2	
DHCO$_3^-$ (m^2 s^{-1})	$9.38 \cdot 10^{-10}$	average from Lin et al. (2003); Wolf et al. (2007)
DPO$_4^{3-}$ (m^2 s^{-1})	$4.16 \cdot 10^{-10}$	average from Liu et al. (2003); Lyons et al. (1982)
DNO$_3^-$ (m^2 s^{-1})	$1.29 \cdot 10^{-9}$	average from Liu et al. (2003); Satoh et al. (2004); Wolf et al. (2007)
$E_{n,PAR,\lambda}$ (nm^{-1}) [b]	Phillips Master PL-L spectrum	Measured
PFD$_{in}$ (µmol m^{-2} s^{-1})	180	Measured during experiment
YN (g biomass g^{-1} N)	12.2	Calculated
YP (g biomass g^{-1} P)	103.5	Calculated
YC (g biomass g^{-1} P)	2.1	Calculated
z	50 steps	Calculated

[a] Data shown in Fig. 10
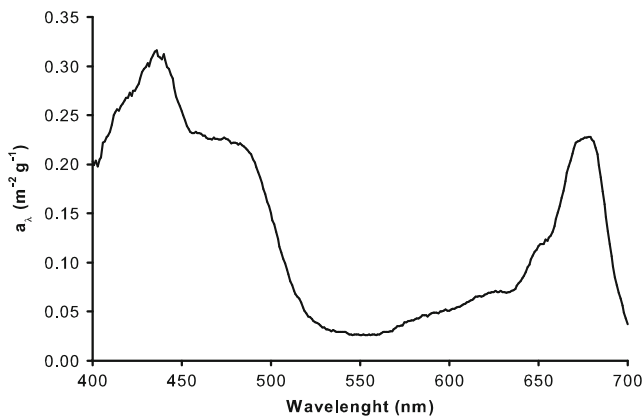
[b] Data shown in Fig. 11

Fig. 11 The specific absorption coefficient (a_λ) for *Chlorella sorokiniana*

assumed no mass transfer limitation occurred at the liquid–biofilm interface.

Penetration of light

The following formula was used to calculate the light intensity at depth z inside the biofilm:

$$\mathrm{PFD}(z) = \sum_{\lambda=400}^{\lambda=700} \left(\mathrm{PFD}_{\mathrm{in}} \cdot E_{n,\mathrm{PAR},\lambda} \cdot e^{-a_\lambda \cdot C_x \cdot z \cdot d} \cdot \Delta\lambda \right) \left[\mu\mathrm{mol}\ \mathrm{m}^{-2}\ \mathrm{s}^{-1} \right]$$

with $\mathrm{PFD}_{\mathrm{in}}$ the photon flux density of the incoming light (picomoles per square meter per second), $E_{n,\mathrm{PAR}\lambda}$ the normalized spectral distribution of the PAR photons (400–700 nm nm^{-1}), a_λ the specific absorption coefficient (square meters per gram), C_x the algae concentration (grams per cubic meter), z the biofilm depth (meters), d a light-path enhancement factor (−), and $\Delta\lambda$ the wavelength interval (nanometers).

Table 6 shows the parameters that were used for this calculation. To obtain the $E_{n,\mathrm{PAR},\lambda}$ for the Phillips Master PL-L lamps for the experiments, the spectral photon flux density was measured using a fiber-optic CCD-based spectroradiometer (AvaSpec-2048 detector, Fiber FC-IR100-1-ME, Avantes, Eerbeek, The Netherlands) at 1-nm intervals (for details on the measurement protocol, see Vejrazka et al. (2011)). This measurement was normalized for the PAR range to obtain the normalized emission spectrum according to the following equation:

$$E_{n,\mathrm{PAR},\lambda} = \frac{\mathrm{PFD}_\lambda}{\mathrm{PFD}} \left[\mathrm{nm}^{-1} \right]$$

with PFD_λ the spectral photon flux density (micromoles per square meter per second per nanometer) and PFD, the photon flux density in the PAR range (400–700 nm, micromoles per square meter per second). Figure 10 shows $E_{n,\mathrm{PAR},\lambda}$ of the Phillips Master PL-L lamps. The a_λ used for phototrophs adapted to high light conditions (top layer of the biofilm) was the a_λ measured for *Chlorella sorokiniana* shown in Fig. 11 (for details on the cultivation see Kliphuis et al. (2010) and for details of the measurement protocol see Vejrazka et al. (2011)). In order to simulate low light adapted phototrophs this a_λ was multiplied with a factor 2.

References

Andersen RA (ed) (2005) Algal culturing techniques. Elsevier Academic Press, San Diego, CA

Biggs BJF (1996) Patterns in benthic algae of streams. In: Stevenson RJ, Bothwell ML, Lowe RL (eds) Algal ecology: freshwater benthic ecosystems. Academic Press Elsevier, London, pp 31–56

Bishop PL, Zhang TC, Fu YC (1995) Effects of biofilm structure, microbial distributions and mass transport on biodegradation processes. Water Sci Technol 31:143–152

Blier R, Laliberte G, de la Nou J (1995) Tertiary treatment of cheese factory anaerobic effluent with *Phormidium bohneri* and *Micractinum pusillum*. Bioresour Technol 52:151–155

Boelee NC, Temmink H, Janssen M, Buisman CJN, Wijffels RH (2011) Nitrogen and phosphorus removal from municipal wastewater effluent using microalgal biofilms. Water Res 45:5925–5933

Boelee NC, Temmink H, Janssen M, Buisman CJN, Wijffels RH (2012) Scenario analysis of nutrient removal from municipal wastewater by microalgal biofilms. Water 4:460–473

Clegg M, Gaedke U, Boehrer B, Spijkerman E (2012) Complementary ecophysiological strategies combine to facilitate survival in the hostile conditions of a deep chlorophyll maximum. Oecologia 169:609–622

De Beer D, Stoodley P, Roe F, Lewandowski Z (1994) Effects of biofilm structures on oxygen distribution and mass transport. Biotechnol Bioeng 43:1131–1138

Duboc P, Marison I, Uv S (1999) Quantitative calorimetry and biochemical engineering. In: Kemp RB (ed) Handbook of thermal analysis and calorimetry vol 4. Elsevier, Amsterdam, pp 287–309

Ellwood NTW, Di Pippo F, Albertano P (2011) Phosphatase activities of cultured phototrophic biofilms. Water Res 46:378–386

Fujimoto N, Sudo R (1997) Nutrient-limited growth of *Microcystis aeruginosa* and *Phormidium tenue* and competition under various N:P supply ratios and temperatures. Limnol Oceanogr 42:250–256

Godos I, González C, Becares E, García-Encina P, Muñoz R (2009) Simultaneous nutrients and carbon removal during pretreated swine slurry degradation in a tubular biofilm photobioreactor. Appl Microbiol Biot 82:187–194

González C, Marciniak J, Villaverde S, León C, García PA, Munoz R (2008) Efficient nutrient removal from swine manure in a tubular biofilm photo-bioreactor using algae-bacteria consortia. Water Sci Technol 58:95–102

Guzzon A, Bohn A, Diociaiuti M, Albertano P (2008) Cultured phototrophic biofilms for phosphorus removal in wastewater treatment. Water Res 42:4357–4367

Healey FP (1973) Inorganic nutrient uptake and deficiency in algae. Crit Rev Microbiol 3:69–113

Hecky RE, Kilham P (1988) Nutrient limitation of phytoplankton in freshwater and marine environments: a review of recent evidence on the effects of enrichment. Limnol Oceanogr 33:796–822

Hill W (1996) Effects of light. In: Stevenson RJ, Bothwell ML, Lowe RL (eds) Algal ecology: freshwater benthic ecosystems. Academic Press Elsevier, London, pp 121–148

Hoehn RC, Ray AD (1973) Effects of thickness on bacterial film. J Water Pollut Control Fed 45:2302–2320

Johnson MB, Wen Z (2009) Development of an attached microalgal growth system for biofuel production. Appl Microbiol Biotechnol 85:525–534

Johnson RE, Tuchman NC, Peterson CG (1997) Changes in the vertical microdistribution of diatoms within a developing periphyton mat. J N Am Benthol Soc 16:503–519

Kliphuis AMJ, de Winter L, Vejrazka C, Martens DE, Janssen M, Wijffels RH (2010) Photosynthetic efficiency of *Chlorella sorokiniana* in a turbulently mixed short light-path photobioreactor. Biotechnol Prog 26:687–696

Lin YH, Leu JY, Lan CR, Lin PHP, Chang FL (2003) Kinetics of inorganic carbon utilization by microalgal biofilm in a flat plate photoreactor. Chemosphere 53(7):779–787

Liu SM, Zhang J, Jiang WS (2003) Pore water nutrient regeneration in Shallow Coastal Bohai Sea, China. J Oceanogr 59:377–385

Lyons WB, Loder TC, Murray SM (1982) Nutrient Pore water chemistry, Great Bay, New Hampshire: Benthic fluxes. Estuaries 5:230–233

Murphy TE, Berberoğlu H (2012) Temperature fluctuation and evaporative loss rate in an algae biofilm photobioreactor. J Sol Energ-T ASME 134:011002.1–011002.9

Morita M, Watanabe Y, Saiki H (2000) High photosynthetic productivity of green microalga *Chlorella sorokiniana*. Appl Biochem Biotechnol 87:203–218

Norsker N-H, Barbosa MJ, Vermuë MH, Wijffels RH (2011) Microalgal production—a close look at the economics. Biotechnol Adv 29:24–27

Ozkan A, Kinney K, Katz L, Berberoglu H (2012) Reduction of water and energy requirement of algae cultivation using an algae biofilm photobioreactor. Bioresour Technol 114:542–548

Posadas E, García-Encina P-A, Soltau A, Domínguez A, Díaz I, Muñoz R (2013) Carbon and nutrient removal from centrates and domestic wastewater using algal–bacterial biofilm bioreactors. Bioresour Technol 139:50–58

Pérez J, Picioreanu C, van Loosdrecht M (2005) Modeling biofilm and floc diffusion processes based on analytical solution of reaction–diffusion equations. Water Res 39:1311–1323

Sabater S, Guasch H, Romaní A, Muñoz I (2002) The effect of biological factors on the efficiency of river biofilms in improving water quality. Hydrobiologia 469:149–156

Satoh H, Ono H, Rulin B, Kamo J, Okabe S, Fukushi K-I (2004) Macro-scale and microscale analyses of nitrification and denitrification in biofilms attached on membrane aerated biofilm reactors. Water Res 38:1633–1641

Sekar R, Nair KVK, Rao VNR, Venugopalan VP (2002) Nutrient dynamics and successional changes in a lentic freshwater biofilm. Freshwat Biol 47:1893–1907

Steinman AD, McIntire CD (1987) Effects of irradiance on the community structure and biomass of algal assemblages in laboratory streams. Can J Fish Aquat Sci 44:1640–1648

Stewart PS (1997) A review of experimental measurements of effective diffusive permeabilities and effective diffusion coefficients in biofilms. Biotechnol Bioeng 59:261–272

Talbot P, Thebault JM, Dauta A, de la Noue J (1991) A comparative study and mathematical modeling of temperature, light and growth of three microalgae potentially useful for wastewater treatment. Water Res 25:465–472

Van Vooren L, Lessard P, Ottoy JP, Vanrolleghem PA (1999) pH Buffer capacity based monitoring of algal wastewater treatment. Environ Technol 20:547–561

Vejrazka C, Janssen M, Streefland M, Wijffels RH (2011) Photosynthetic efficiency of *Chlamydomonas reinhardtii* in flashing light. Biotechnol Bioeng 108:2905–2913

Wäsche S, Horn H, Hempela DC (2002) Influence of growth conditions on biofilm development and mass transfer at the bulk/biofilm interface. Water Res 36:4775–4784

Wolf G, Picioreanu C, van Loosdrecht MCM (2007) Kinetic modeling of phototrophic biofilms: The PHOBIA model. Biotechnol Bioeng 97:1064–1079

Zippel B, Neu TR (2005) Growth and structure of phototrophic biofilms under controlled light conditions. Water Sci Technol 52:203–209